Check for updates

Geophysical Research Letters

RESEARCH LETTER
10.1029/2024GL111388

In Situ Aerosol Size Spectra Measurements in the Austral Polar Vortex Before and After the Hunga Tonga-Hunga Ha'apai Volcanic Eruption

Terry Deshler[1], Lars E. Kalnajs[1], Matthew Norgren[1], Yunqian Zhu[2], and Jun Zhang[3]

[1]Laboratory for Atmospheric and Space Physics, University of Colorado, Boulder, CO, USA, [2]University of Colorado Cooperative Institute for Research in Environmental Sciences (CIRES) at the NOAA Chemical Sciences Laboratory, Boulder, CO, USA, [3]Atmospheric Chemistry Observations & Modeling Laboratory, National Center for Atmospheric Research, Boulder, CO, USA

Key Points:

- Austral polar vortex aerosol concentrations from Hunga Tonga increased, for particles >0.5 μm, by factors of 2–5 below, >10 above, 18 km
- Concomittant increases in SO_4 mass, surface area, and near IR extinction were by factors of 2–4 below, and 5–10 above, 18 km
- Effective radius, with radiative and microphysical implications, increased from ∼0.2 to ∼0.3 μm at the peak of the layer

Correspondence to:

T. Deshler,
deshler@uwyo.edu

Citation:

Deshler, T., Kalnajs, L. E., Norgren, M., Zhu, Y., & Zhang, J. (2024). In situ aerosol size spectra measurements in the austral polar vortex before and after the Hunga Tonga-Hunga Ha'apai volcanic eruption. *Geophysical Research Letters*, *51*, e2024GL111388. https://doi.org/10.1029/2024GL111388

Received 19 JUL 2024
Accepted 3 NOV 2024

© 2024. The Author(s).
This is an open access article under the terms of the Creative Commons Attribution-NonCommercial-NoDerivs License, which permits use and distribution in any medium, provided the original work is properly cited, the use is non-commercial and no modifications or adaptations are made.

Abstract Aerosol from the Hunga Tonga-Hunga Ha'apai (HT-HH) volcanic eruption (20.6°S) in January 2022 were not incorporated into the austral polar vortex until the following year, March 2023. Within the polar vortex in situ profiles of aerosol size spectra were completed in the austral autumns of 2019 and 2023, from McMurdo Station, Antarctica (78°S), 30 months prior to and 15 months after the HT-HH eruption. The measurements indicate that the HT-HH impact on aerosol size was primarily confined to particles with diameters >0.5 μm leading to differences in aerosol mass, surface area, and extinction from factors of 2–4 at the volcanic layer's peak below 20 km, increasing to ratios of 5–10 above 20 km. Effective radius, with radiative and microphysical implications, increased from ∼0.2 to ∼0.3 μm. An Earth system model with a modal aerosol package compares favorably with the in situ measurements of the HT-HH aerosol impact.

Plain Language Summary In austal autumn of 2019 and 2023 balloon-borne measurements of aerosol size distributions were completed above McMurdo Station, Antarctica (78°S, 167°E). Size spectra were measured for particles between 0.01 and 16 μm from the surface to over 30 km. Between these two sets of measurements the Hunga Tonga-Hunga Ha'apai (HT-HH) volcano (20.6°S) started an eruptive phase culminating with a massive underwater explosion on 15 January 2022. Due to the timing of the eruption, the HT-HH volcanic aerosol were not incorporated into the austral polar vortex until 2023, which formed about a month before the 2023 aerosol measurements were completed. The 2019 measurements were in a volcanically quiescent period and capture the background stratospheric aerosol. The two sets of measurements are used to characterize the impact of HT-HH on stratospheric aerosol within the austral polar vortex, particularly on quantities important for assessing the volcanic impact on climate and heterogeneous chemistry: aerosol mass, surface area, and light extinction. Such quantities were observed to increase by factors of 2–4 below, and 5–10 above, 20 km after the eruption. An Earth System Model with an aerosol package compared favorably wih the measurements. Polar ozone loss in 2023 was, however, not impacted significantly.

1. Introduction

The Hunga Tonga-Hunga Ha'apai (HT-HH) volcano (20.6°S, 175.4°W) started an eruptive phase on 20 December 2021 which culminated with a massive underwater explosion on 15 January 2022. Aerosol from the final eruption were estimated to reach above 50 km (Carr et al., 2022; Proud et al., 2022). Due to its location, 150 m below sea level (Cronin et al., 2017), significant amounts of water were injected along with sulfur and ash. Microwave Limb Sounder (MLS) measurements from the AURA satellite indicate ∼150 Tg of water was injected, approximately 10% of the normal stratospheric burden (Millán et al., 2022). In contrast, the estimates of SO_2 suggest a modest injection, ∼0.5 Tg (Carn et al., 2022; Witze, 2022). Aerosol layers were observed at 38 km over Australia a few days after the eruption by the Ozone Mapping and Profiling Suite Limb Profiler (OMPS-LP) (Taha et al., 2022) and over Reunion Island at 36 km after 4 days and at 28 km after 7 days (Khaykin et al., 2022). Cloud-Aerosol Lidar with Orthogonal Polarization (CALIOP) observations one day after the eruption showed a significant contribution from depolarizing non-spherical particles between 35 and 40 km, but this was short lived and likely to be ash. The CALIOP pass the following day showed little depolarization (Sellitto et al., 2022), indicating fast descent of the upper plume which may have been caused by significant radiative cooling associated with the excess water vapor at these altitudes (Sellitto et al., 2022). In contrast most volcanic aerosol plumes are self-lofted initially due to absorption of terrestrial infra-red by the sulfate aerosol (e.g., Fairlie et al., 2017). The stratospheric

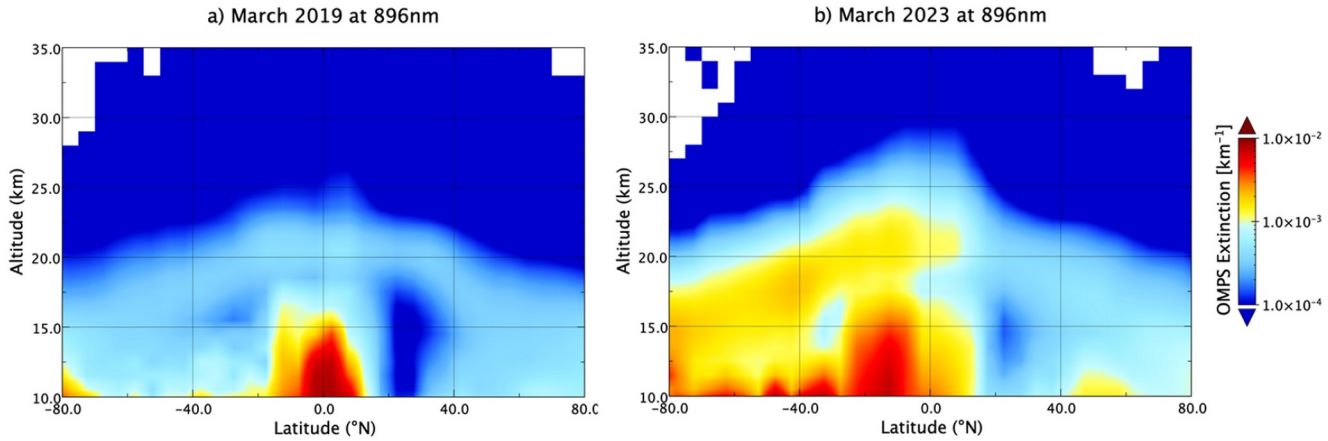

Figure 1. Latitude and altitude cross section of OMPS-LP average monthly measurements of aerosol extinction coefficient at 896 nm (km^{-1}) along a longitude of 167°E for (a) March 2019 and (b) March 2023. After March the OMPS single scattering angle begins to limit high latitude measurements.

water appears to have led to abundant OH and thus halving the SO_2 lifetime compared to a case without water injection (Asher et al., 2023; Zhu et al., 2022). The HT-HH eruption is unique due to the height of the injection and the low amount of SO_2. Within a month the aerosol had settled into a layer confined between 23 and 26 km and then descended to just above 20 km after 6 months (Legras et al., 2022). The southern extent of this layer was near 60°S by October (Khaykin et al., 2022) and appears to have not entered the polar vortex in 2022 (Manney et al., 2023).

Early in situ measurements indicated that the concentration of all particle sizes <1 μm diameter were enhanced within the HT-HH plumes near 20 km over Reunion Island within a week of the eruption (Kloss et al., 2022). As the plume aged these smaller particles appear to have been lost to the larger particles. A measurement at 24 km above the Tibetan plateau in April 2022 showed that concentrations enhanced by HT-HH were primarily for particles >0.6 μm (Bian et al., 2023). By early 2023 the southern hemispheric dispersal and altitude coalescence of the HT-HH aerosol appeared complete (Taha et al., 2022). Monthly averages of OMPS-LP profiles in March 2019 and 2023, Figure 1, show that HT-HH aerosol had reached >85°S by April 2023, and thus HT-HH aerosol and its associated water would have been incorporated into the Antarctic polar vortex; however, the impact of these quantities on 2023 polar ozone loss was minimal (Wohltmann et al., 2024; Zhou et al., 2024).

Prior to the eruption of HT-HH, two sets of in situ aerosol profile measurements within the austral autumn polar vortex were planned to address three scientific questions: (a) Does a new particle layer form in austral fall, similar to the one which regularly forms in austral spring (Campbell & Deshler, 2014). Such an austral fall layer was predicted by WACCAM/CARMA (Campbell et al., 2014). (b) Are there early onset PSCs, predicted by (Lambert et al., 2016) based on MLS HNO_3 measurements, which are not observable by CALIOPI? (c) What is the extent of meteoric influence on aerosol entering the polar vortex above 35 km?

The first set of measurements was completed in April 2019, but due to Covid the second set was delayed to April 2023. Thus the measurement set bracketed the HT-HH eruption. These in situ measurements are here compared to illustrate the impact of the HT-HH eruption on stratospheric aerosol within the polar vortex. Concerning the science questions above, (a) and (b) are still works in progress, while (c) is partially answered by Norgren et al. (2024).

2. Measurements, Methods and Results

In the mid 2010s fall and winter season air transport to McMurdo Station, Antarctica (77.8°S, 166.7°E) commenced. This provided the opportunity to make in situ balloon-borne measurements of stratospheric aerosol, both total and size resolved measurements, in austral autumn and winter to investigate new particle formation events and the character of early onset polar stratospheric clouds (PSCs). The first field observations were from late April to mid-June 2019, a period with relatively little stratospheric impacts from volcanism or wildfires. Due to COVID restrictions further field work was fortuitously postponed until April 2023, a little over a year after the

19448007, 2024, 22, Downloaded from https://agupubs.onlinelibrary.wiley.com/doi/10.1029/2024GL111388 by Ripon College Lane Library, Wiley Online Library on [20/12/2024]. See the Terms and Conditions (https://onlinelibrary.wiley.com/terms-and-conditions) on Wiley Online Library for rules of use; OA articles are governed by the applicable Creative Commons License

19448007, 2024, 22, Downloaded from https://agupubs.onlinelibrary.wiley.com/doi/10.1029/2024GL111388 by Ripon College Lane Library, Wiley Online Library on [20/12/2024]. See the Terms and Conditions (https://onlinelibrary.wiley.com/terms-and-conditions) on Wiley Online Library for rules of use; OA articles are governed by the applicable Creative Commons License

eruption of HT-HH in January 2022, which was ample time for the HT-HH aerosol to be incorporated into the 2023 polar vortex.

The instruments deployed during both field campaigns were the stratospheric total aerosol counter (STAC) (Norgren et al., 2024) and the LASP optical particle counter (LOPC) (Kalnajs & Deshler, 2022). STAC measures the concentration of all particles nominally >0.01 μm diameter, while the LOPC is a size spectrometer measuring particles >0.3–8.0 μm diameter in 23 channels. Both of these instruments compare well to University of Wyoming legacy size spectrometers (Deshler et al., 2019) and total aerosol counters (Campbell & Deshler, 2014; Norgren et al., 2024), and to solar extinction at 525 and 1,020 nm wavelength from SAGE III-ISS, as discussed in (Kalnajs & Deshler, 2022).

These aerosol measurements also provide an opportunity for comparison with a numerical experiment conducted using the Community Earth System Model Version 2 (CESM2) Whole Atmosphere Community Climate Model Version 6 (WACCM6), a state-of-the-art chemistry-climate model extending to ∼140 km. Aerosols are represented in a prognostic modal aerosol model (MAM) from which aerosol physical properties can be derived (Mills et al., 2016). The simulations were conducted with a horizontal resolution of 0.9° latitude, 1.25° longitude, and vertical resolution of ∼0.5 km to the mid stratosphere. WACCM6 is operated in a specified dynamics configuration, based on the Modern-Era Retrospective analysis for Research and Applications Version 2 (MERRA-2) reanalysis data (Gelaro et al., 2017), running from 2007 until 2023, utilizing initial conditions from a long historical simulation (Gettelman et al., 2019) incorporating major volcanic eruptions. For the HT-HH eruption, emissions described by Zhu et al. (2022) were used: 150 Tg of H_2O and 0.42 Tg of SO_2 injected on 15 January 2022, from 20 to 35 km. Further details on the model setup can be found in Zhang et al. (2024). The confidence in prognostic aerosol models is enhanced through comparisons with detailed microphysical measurements in remote locations, such as described here.

Figure 2 presents profile measurements from LOPCs flown on 8 June 2019, and 24 April 2023, and from STACs flown on 26 May 2019, and 26 April 2023. The June flight in 2019 was the only LOPC flight not influenced by early season PSCs. The April date in 2023 was dictated by logistical constraints. Both measurements, however, were well within the polar vortex, and the temperatures measured in 2019 are consistent with the absence of PSCs, Figure 2c). Figure 2a) presents the total aerosol concentration and cumulative concentrations at 6 sizes, indicated in the legend, between 0.01 and 1.5 μm diameter with solid (dotted) lines representing the 2019 (2023) measurements. Striking features of this comparison are the rough similarity of concentrations at all sizes in the troposphere, then the significant divergence of concentrations at $d > 0.5$ μm as the instruments enter the stratosphere near 10 km. This point is further emphasized in Figure 2b) showing the ratio of the 2023 to the 2019 measurements. At 0.3 μm the ratio remains near 1.0 up to 22 km, whereas at 0.5 μm and larger, the ratio exceeds two increasing to over an order of magnitude above 18 km, where they remain to the top of the sounding. Meanwhile the ratio of total aerosol concentration remains near 1.0 throughout the profile.

Figure 3 illustrates the size difference further by comparing differential size distributions, directly from the measured data, and from log normal fits to the data (Deshler et al., 2019), for the 2019 and 2023 measurements at 19 km. The size distribution in 2019 is unimodal while in 2023 it is bimodal. The difference is further emphasized in Figure 3b) displaying the distribution of differences in the observed and fitted dN/dlog(D) across the size range of the measurements for 2023–2019. To provide a perspective on the impact of the HT-HH eruption, and on the range possible for stratospheric aerosol, also included on Figure 3a) are the average and standard deviation of aerosol, between 18 and 20 km above Laramie, Wyoming (41°N, 106°W), 15 months after the Pinatubo eruption. Pinatubo injected over 20 times the SO_2 as HT-HH, and this ratio is reflected in the SO_4 masses listed in the legend following the measurement date in Figure 3a), calculated from integrals of the size distributions. The SO_4 masses are given as parts per billion by mass (ppbm) of SO_4 to air. The Pinatubo aerosol shows a significantly larger peak in the second mode dN/dlog(D) yet smaller second mode median radius compared to HT-HH. In the first mode the dN/dlog(D) peaks are similar yet the Pinatubo median radius is a factor of four or so larger.

This comparison illustrates, perhaps, the range of impacts on stratospheric aerosol size spectra arising from a wide range of SO_2 injections, and differing conversion rates for SO_2 to sulfate aerosol. The HT-HH aerosol, with its rapid aerosol formation, e-folding time of 12 days for SO_2, led to high aerosol concentrations which coagulated and grew to large particles with ultimately minimal impact on fine mode aerosol. The 2019 and 2023 fine mode differential distributions have similar median radii and concentrations. The Pinatubo fine mode has a much larger

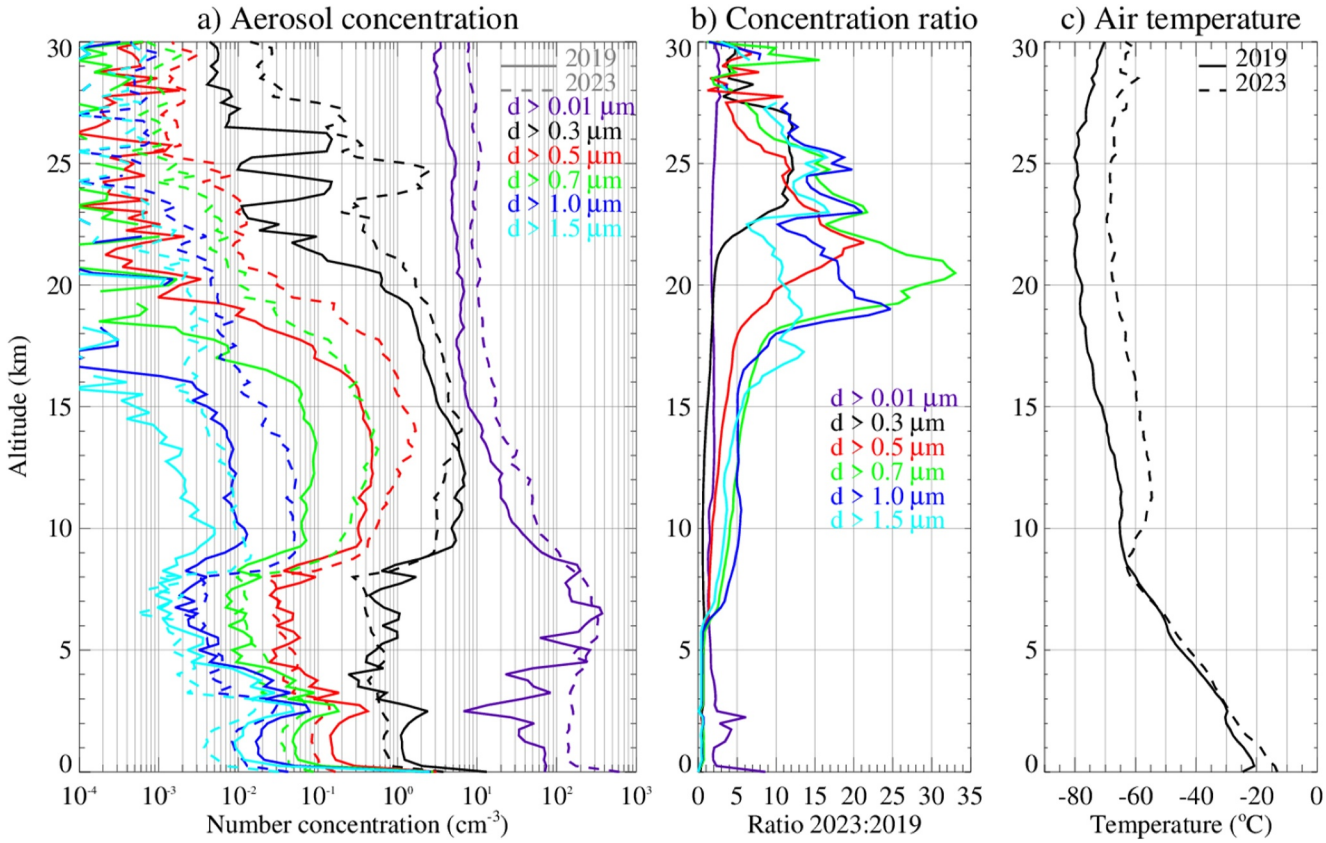

Figure 2. (a) Altitude profile of LOPC aerosol cumulative concentration measurements, at 5 diameters, above McMurdo Station, Antarctica, on 20190608 (solid lines) and 20230424 (dotted lines). Total aerosol concentrations, labeled $d > 0.01$ µm (purple) are from STAC flights on 20190526 and 20230426. (b) Ratios of the concentrations at each size for 2023:2019. (c) Temperature profile for 2019 (solid) and 2023 (dotted).

median radius, although the peak concentrations are similar to HT-HH. This may be reflective of coagulation which limits total aerosol concentrations after a short period of time. In the case of Pinatubo, after the initial impact of coagulation, the fine mode particles continued to grow by condensation due to the much larger SO_2 injection and the slower rate of its conversion to sulfuric acid. The SO_2 e-folding time for Pinatubo was 30–40 days (Carn et al., 2016).

In the coarse mode the HT-HH aerosol are larger but have concentration three orders of magnitude smaller than Pinabuto. For Pinatubo there was evidence of new particle formation (Deshler et al., 1992). With a higher initial small particle concentration, coagulation would have led to more particles transitioning to the larger sizes than for HT-HH, leading to the higher concentrations. With more particles to take up the sulfuric acid individual particle growth would have been smaller than HT-HH. Measurements from Laramie were used for this comparison since there were no pre-winter measurements from McMurdo in this time frame, and the late winter measurements, which are available, are perturbed by PSCs.

The measured size distributions, for example Figure 3, are used to calculate profiles of aerosol moments: SO_4 mass mixing ratio (SMMR), surface area density (SAD), effective radius, extinction coefficient (ExtC). This can be done directly by integrating the size distributions, or through fitting a uni/bi-modal lognormal size distribution to the measurements, Figure 3. The results of either method are similar. Here direct integration of the size distributions are used. The SO_4 mass mixing ratio is obtained from the aerosol volume by calculating the temperature/pressure dependent weight fraction of H_2SO_4 (Hanson et al., 1994; Steele & Hamill, 1981) and the temperature dependent solution density (Luo et al., 1996) to then obtain the SO_4 mass mixing ratio. These calculations are slightly dependent on the water vapor mixing ratio. According to MLS measurements near McMurdo in May 2019 the water vapor mixing ratio was near 5 ppmv up to about 25 km then increased to 7–8

19448007, 2024, 22, Downloaded from https://agupubs.onlinelibrary.wiley.com/doi/10.1029/2024GL111388 by Ripon College Lane Library, Wiley Online Library on [20/12/2024]. See the Terms and Conditions (https://onlinelibrary.wiley.com/terms-and-conditions) on Wiley Online Library for rules of use; OA articles are governed by the applicable Creative Commons License

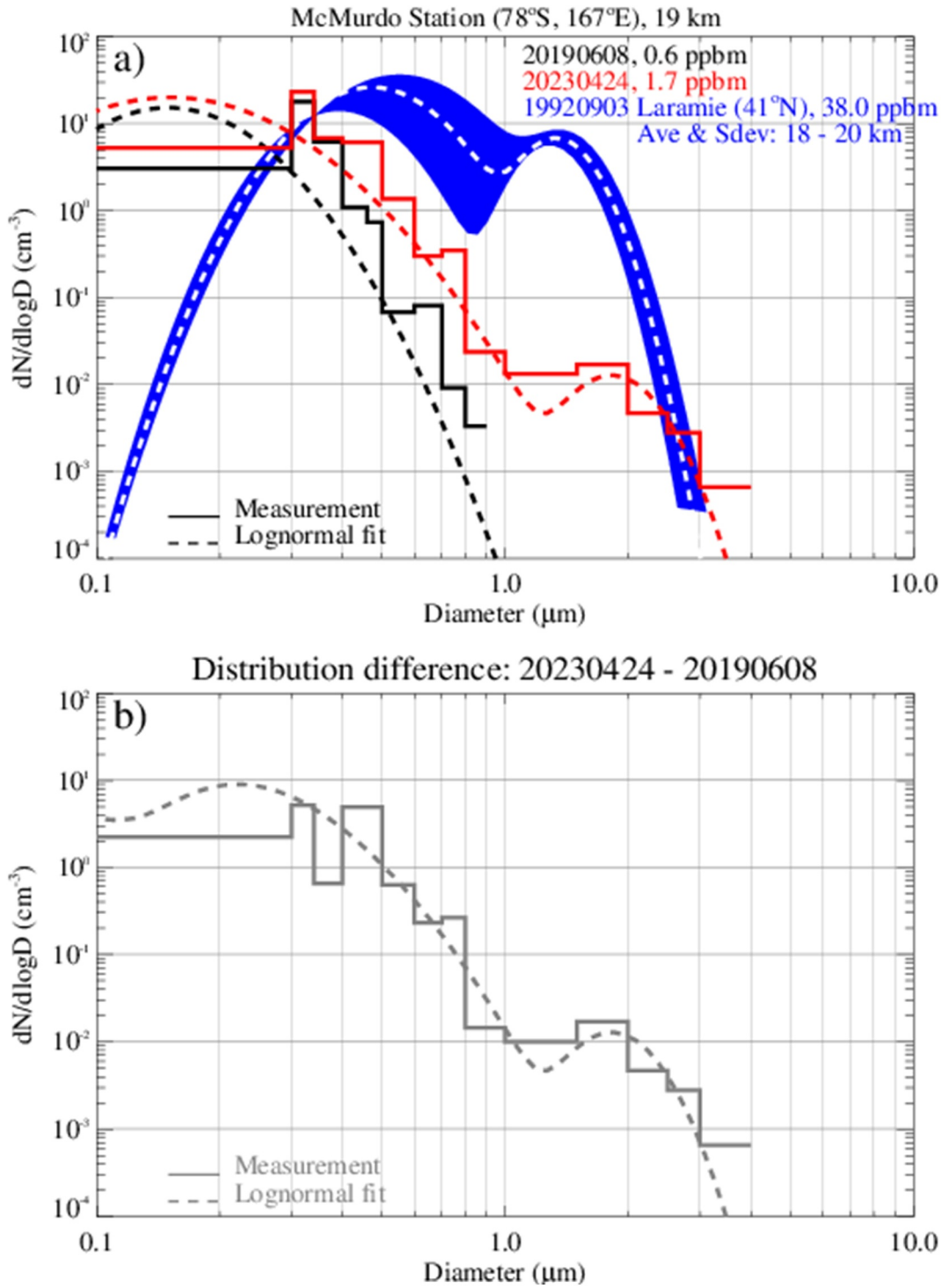

Figure 3. (a) Differential size distributions for particles from 0.01 to 8 μm diameter for both the measurements (solid) and fitted size distributions (dashed) at 19 km on 20190608 (black), 20230424 (red), and 19920903 (blue shading) from Laramie, Wyoming 15 months after the Pinatubo eruption. (b) Difference between the measured and fitted size distributions for 20230424–20190608. The SO_4 mass, in ppbm, from integrating the size distributions is shown in the legend in (a).

near 30 km. In late April 2023 the MLS measured water vapor was higher, near 7 ppmv above 18 km, and remained there up to 30 km. For the calculations here the water vapor is held constant at 5 and 7 ppmv for 2019 and 2023. Such differences have little impact on mass mixing ratio or extinction.

19448007, 2024, 22, Downloaded from https://agupubs.onlinelibrary.wiley.com/doi/10.1029/2024GL111388 by Ripon College Lane Library, Wiley Online Library on [20/12/2024]. See the Terms and Conditions (https://onlinelibrary.wiley.com/terms-and-conditions) on Wiley Online Library for rules of use; OA articles are governed by the applicable Creative Commons License

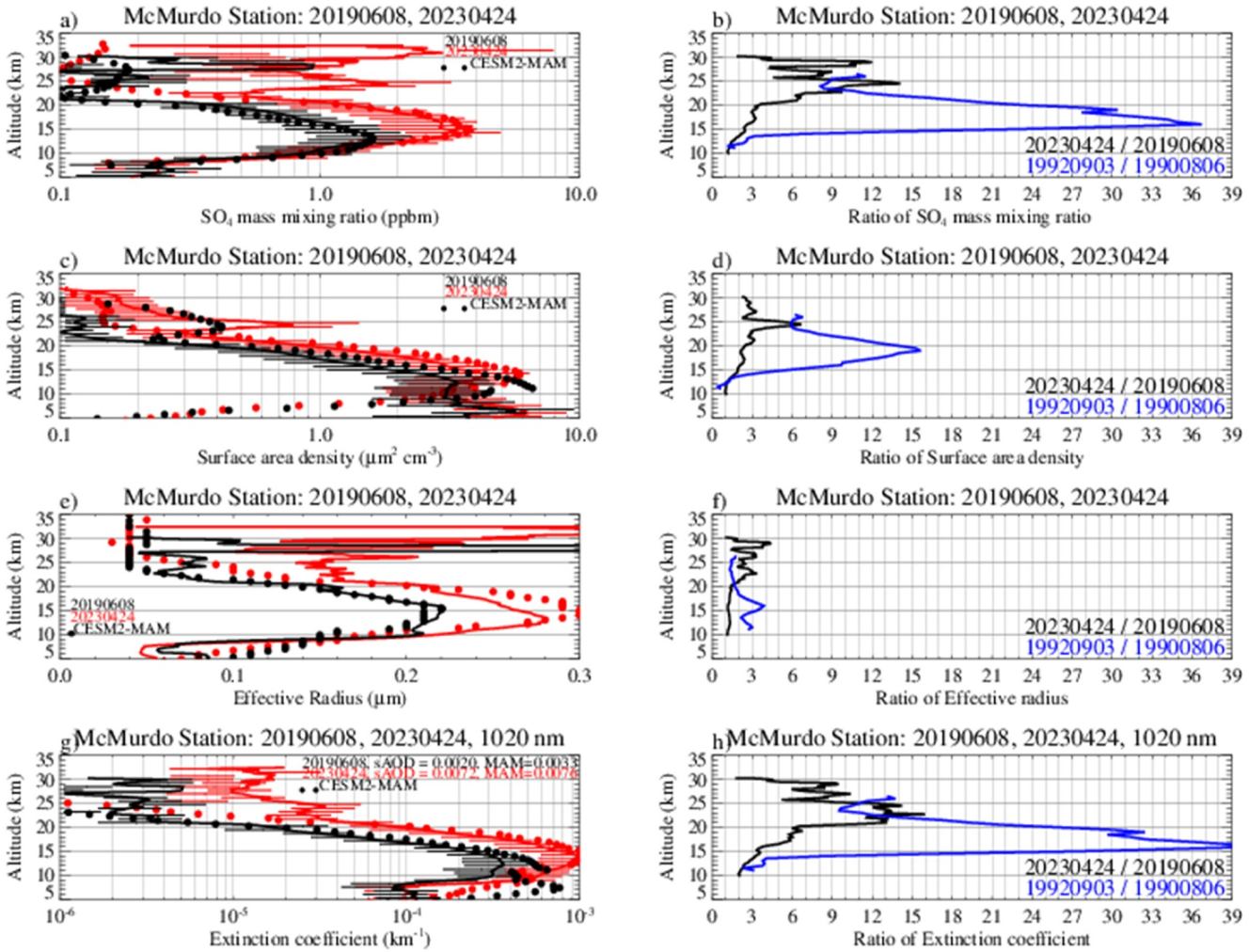

Figure 4. Altitude profiles of (a) SO_4 mass mixing ratio (ppbm), (c) surface area density ($\mu m^2\ cm^{-3}$), (e) effective radius (μm), and (g) extinction at 1,020 nm (km^{-1}), derived from the in situ measurements (solid with horizontal bars) and the numerical experiments (dotted), for 20190608 (black) and 20230424 (red). The horizontal bars on (a), (c), and (g) represent ±40% uncertainty associated with moments of the in situ size spectra. Altitude profiles of the ratios 2023:2019 of each of these quantities are shown in (b), (d), (f) and (h). The 1,020 nm sAOD is shown in panel (g) legend. Also in (b), (d), (f), and (h) are ratios of measurements from 19920903: 19900806, 15 months after, and one year before, the Pinatubo eruption, from Laramie, Wyoming (41°N, 106°W) in blue.

The post HT-HH measurements show a significant and consistent enhancement across a range of aerosol properties. Figure 4 shows, for 2019 and 2023 estimates of SMMR, SAD, effective radius, and ExtC at 1,020 nm (a, c, e, g). The horizontal bars represent the ±40% uncertainty associated with the moments of OPC size distributions (Deshler et al., 2003). The ratios, post to pre HT-HH, of SMMR and SAD are shown in Figures 4b and 4d) and tell a similar story. Both ratios start near 1 at 10 km, just above the tropopause, and then increase to a ratio near 3 at 20 km, similar to the concentration ratios for particles ≥0.5 μm up to about 18 km. Above 20 km the concentration ratios at all sizes except 0.3 μm increase to between 10 and 20, Figure 2b). In Figures 4b and 4d) the SMMRs increase to the 5–10 range, while SAD increases remain in the 2.5–3 range. This is a region where there are only a few particles at the larger sizes, particularly in 2019. Post HT-HH, the effective radii increase by roughly a factor of 1.3 up to 20 km and then a factor of 2–3 increase above 20 km, Figure 4e 4f), somewhat similar to SAD. The ratios of ExtC are similar to the differences in mass. The stratospheric aerosol optical depth (sAOD), Figure 4g), doubles from 0.002 (0.0033) to 0.0072 (0.0076) for observations (model) from 2019 to 2023. The consistency of the LOPC measurements below 10 km in 2019 and 2023 are striking, Figures 2 and 4, suggesting little inter-annual variation in tropospheric aerosol near McMurdo Station.

Calculations of the same quantities from the CESM2-MAM model are shown as color coded dots on each of the left hand panels for Figure 4. In general the model estimates agree well with the observations in the HT-HH

19448007, 2024, 22, Downloaded from https://agupubs.onlinelibrary.wiley.com/doi/10.1029/2024GL111388 by Ripon College Lane Library, Wiley Online Library on [20/12/2024]. See the Terms and Conditions (https://onlinelibrary.wiley.com/terms-and-conditions) on Wiley Online Library for rules of use; OA articles are governed by the applicable Creative Commons License

19448007, 2024, 22, Downloaded from https://agupubs.onlinelibrary.wiley.com/doi/10.1029/2024GL111388 by Ripon College Lane Library, Wiley Online Library on [20/12/2024]. See the Terms and Conditions (https://onlinelibrary.wiley.com/terms-and-conditions) on Wiley Online Library for rules of use; OA articles are governed by the applicable Creative Commons License

aerosol layer peak between 10 and 20 km and in the pre HT-HH aerosol in 2019. MAM significantly underestimates the observations above 22 km for all quantities in 2023, but is mostly in agreement at these altitudes in 2019. MAM significantly overestimates SAD and ExtC between 10 and 15 km in 2019. The underestimation of the aerosol above 20 km in 2023, and the origin of these aerosol is unexplained; however, 15 months after the eruption most of the HT-HH aerosol was confined to below 20 km, particularly at high southern latitudes, Figure 1.

Expanding on the Pinatubo comparison in Figure 3, comparisons were made between Laramie stratospheric aerosol measurements 1 year prior to and 15 months after the Pinatubo eruption. The measurements were used to calculate the quantities displayed in Figure 4 and to form ratios of post: pre Pinatubo eruption for each quantity. These are shown in Figures 4b), d), f) and h) in blue. Comparing the post: pre volcanic aerosol ratios for the two eruptions, at the peak of the layer between 15 and 20 km, indicate, for SMMR, SAD, effective radius, and ExtC, that the impact of Pinatubo was larger by factors reaching roughly 10, 8, 3, and 6 respectively. None of these differences, 15 months after the eruption, are proportional to the difference in estimates of Pinatubo sulfur injections which are over 20 times higher than HT-HH. Li et al. (2024) point out that despite a factor of 10 difference in global sAOD between the eruptions of HT-HH and Pinatubo, the sAOD normalized by the SO_2 emission indicates the HT-HH aerosol was twice as effective at impacting solar radiation as Pinatubo. Applying such an SO_2 normalization to the ratios of ExtC shown in Figure 4h) leads to a similar conclusion, as the ratios would be normalized by the HT-HH and Pinatubo injections of 0.5 and 12 Tg SO_2. Li et al. (2024) also point out that the higher sAOD effectivity of HT-HH results partly from the dependence of extinction efficiency on radius.

The peak in solar extinction efficiency for particles <1.0 μm is near a particle radius of 0.3 μm. The sAOD is the integral of extinction over the stratosphere, while extinction is proportional to the aerosol cross section times the Mie scattering cross section, or extinction efficiency. Thus the particle size most important for extinction is the average of particle size weighted by the particle cross section, or the effective radius. For HT-HH the effective radius, 0.28 μm, is very near the peak in the extinction efficiency curve, while for Pinatubo the effective radius is 0.5–0.6 μm where the extinction efficiency is lower. The other factor that Li et al. point to as contributing to the difference is the higher injection altitude from HT-HH compared to Pinatubo. That difference is not apparent in these polar measurements.

Despite significant differences in the injection of water vapor and SO_2 between Pinatubo and HT-HH and the time frame for initial aerosol formation, the aged aerosol exhibit some similarities in their size distributions. Although the Pinatubo aerosol first mode median radius is 3 times larger than that from HT-HH, the peaks in first mode differential size distribution are similar. In contrast, the HT-HH second mode median radius is larger than that from Pinatubo by about 50%, but the peaks in second mode differential size distribution differ by nearly a 1,000.

3. Conclusions

In situ profiles of aerosol size spectra were completed in the austral autumns of 2019 and 2023 from McMurdo Station, Antarctica, 30 months prior and 15 months following the HT-HH eruption in January 2022. The measurements indicate that the HT-HH impact on size was primarily confined to particles ≥0.5 μm, which has also been noted in the Northern Hemisphere about 4 months after the eruption (Bian et al., 2023). These size differences led to pronounced differences in aerosol SO_4 mass mixing ratio, surface area density, and extinction coefficient from factors of 2–4 between 10 and 20 km, the location of the predominant aerosol layer. At the layer peak, 15 km, the SO_4 mass mixing ratio was ∼3 ppbm, surface area density ∼5 $\mu m^2\ cm^{-3}$, effective radius 0.28 μm and extinction coefficient, at 1,020 nm, 0.001 km^{-1}. The stratospheric aerosol optical depth was observed to increase from 0.002 in 2019 to 0.007 in 2023. Differences above 20 km were more pronounced, doubled or more, but not as uniform. Each of these quantities was also available from a numerical experiment completed using CESM2-WACCM6 incorporating a modal aerosol model. The model and observations agreed well below 20 km where the impact of the HT-HH aerosol was most clearly observed, providing confidence that the model is adequately representing aerosol physics. Comparisons made with Pinatubo aerosol in the northern hemisphere, at a similar time post eruption, indicate volcanic impacts on stratospheric aerosol burden in the range of 5–10 times the impact of HT-HH. But this comparison also indicates that, for sAOD normalized by SO_2 emission, the HT-HH aerosol was about twice as effective as the Pinatubo aerosol in causing light extinction. This is partly attributed to the smaller effective radius characteristic of HT-HH compared to Pinatubo.

Data Availability Statement

The in situ balloon-borne data are hosted at the Univeristy of Wyoming digital archves (Deshler, 2023). The OMPS-LP data (Taha et al., 2022) are archived at NASA's Earthdata archive (Taha, 2022). The model data set (Zhang et al., 2024) is available at Jinpeng (2022). Software used for figure creation is at (Deshler & Kalnajs, 2024).

Acknowledgments
The in situ measurements were funded by the US National Science Foundation under award 1745008. Gratitude is also extended to the field support provided by the personnel at McMurdo Station, Antarctica.

References

Asher, E., Todt, M., Rosenlof, K., Thornberry, T., Gao, R.-S., Taha, G., et al. (2023). Unexpectedly rapid aerosol formation in the Hunga Tonga plume. *Proceedings of the National Academy of Sciences*, *120*(46), e2219547120. https://doi.org/10.1073/pnas.2219547120

Bian, J., Li, D., Bai, Z., Xu, J., Li, Q., Wang, H., et al. (2023). First detection of aerosols of the Hunga Tonga eruption in the Northern Hemisphere stratospheric westerlies. *Scientific Bulletin*, *68*(6), 574–577. https://doi.org/10.1016/j.scib.2023.03.002

Campbell, P., & Deshler, T. (2014). Condensation nuclei measurements in the midlatitude (1982-2012) and Antarctic (1986-2010) stratosphere between 20 and 35 km: Condensation nuclei in the stratosphere. *Journal of Geophysical Research: Atmospheres*, *119*(1), 137–152. https://doi.org/10.1002/2013JD019710

Campbell, P., Mills, M., & Deshler, T. (2014). The global extent of the mid stratospheric CN layer: A three-dimensional modeling study. *Journal of Geophysical Research: Atmospheres*, *119*(2), 1015–1030. https://doi.org/10.1002/2013JD020503

Carn, S. A., Clarisse, L., & Prata, A. J. (2016). Multi-decadal satellite measurements of global volcanic degassing. *Journal of Volcanology and Geothermal Research*, *311*, 99–134. https://doi.org/10.1016/j.jvolgeores.2016.01.002

Carn, S. A., Krotkov, N. A., Fisher, B. L., & Li, C. (2022). Out of the blue: Volcanic SO2 emissions during the 2021–2022 eruptions of Hunga Tonga—Hunga Ha'apai (Tonga). *Frontiers in Earth Science*, *10*. https://doi.org/10.3389/feart.2022.976962

Carr, J. L., Horváth, Á., Wu, D. L., & Friberg, M. D. (2022). Stereo plume height and motion retrievals for the record-setting Hunga Tonga-Hunga Ha'apai eruption of 15 January 2022. *Geophysical Research Letters*, *49*(9), e2022GL098131. https://doi.org/10.1029/2022GL098131

Cronin, S. J., Brenna, M., Smith, I. E. M., Barker, S. J., Tost, M., Ford, M., et al. (2017). New volcanic island unveils explosive past. *Eos*, *98*. Published on. https://doi.org/10.1029/2017EO076589 26 June 2017.

Deshler, T. (2023). University of Wyoming stratospheric aerosol measurements [Dataset]. *University of Wyoming. Collection*. https://doi.org/10.15786/c.6379371.v1

Deshler, T., Hervig, M. E., Hofmann, D. J., Rosen, J. M., & Liley, J. B. (2003). Thirty years of in situ stratospheric aerosol size distribution measurements from Laramie, Wyoming (41°N), using balloon-borne instruments. *Journal of Geophysical Research*, *108*(D5). https://doi.org/10.1029/2002JD002514

Deshler, T., Hofmann, D. J., Johnson, B. J., & Rozier, W. R. (1992). Balloonborne measurements of the Pinatubo aerosol size distribution and volatility at Laramie, Wyoming during the summer of 1991. *Geophysical Research Letters*, *19*(2), 199–202. https://doi.org/10.1029/91gl02787

Deshler, T., & Kalnajs, L. (2024). HT-HH austral polar observations [Software]. *OSF*. https://doi.org/10.17605/OSF.IO/ZEMVN

Deshler, T., Luo, B., Kovilakam, M., Peter, T., & Kalnajs, L. E. (2019). Retrieval of aerosol size distributions from in situ particle counter measurements: Instrument counting efficiency and comparisons with satellite measurements. *Journal of Geophysical Research: Atmospheres*, *124*(9), 5058–5087. https://doi.org/10.1029/2018JD029558

Fairlie, T. D., Vernier, J.-P., Natarajan, M., & Bedka, K. M. (2014). Dispersion of the Nabro volcanic plume and its relation to the Asian summer monsoon. *Atmospheric Chemistry and Physics*, *14*(13), 7045–7057. https://doi.org/10.5194/acp-14-7045-2014

Gelaro, R., McCarty, W., Suárez, M. J., Todling, R., Molod, A., Takacs, L., et al. (2017). The Modern-Era Retrospective analysis for Research and Applications, version 2 (MERRA-2). *Journal of Climate*, *30*(14), 5419–5454. https://doi.org/10.1175/JCLI-D-16-0758.1

Gettelman, A., Mills, M. J., Kinnison, D. E., Garcia, R. R., Smith, A. K., Marsh, D. R., et al. (2019). The Whole Atmosphere community climate model version 6 (WACCM6). *Journal of Geophysical Research: Atmospheres*, *124*(23), 12380–12403. https://doi.org/10.1029/2019JD030943

Hanson, D. R., Ravishankara, A. R., & Solomon, S. (1994). Heterogeneous reactions in sulfuric acid aerosols: A framework for model calculations. *Journal of Geophysical Research*, *99*(D2), 3615–3629. https://doi.org/10.1029/93JD02932

Jinpeng, L. (2022). Model description [Dataset]. *Figshare*. https://doi.org/10.6084/m9.figshare.21652358

Kalnajs, L. E., & Deshler, T. (2022). A new instrument for balloon-borne in situ aerosol size distribution measurements, the continuation of a 50 Year record of stratospheric aerosols measurements. *Journal of Geophysical Research: Atmospheres*, *127*(24), e2022JD037485. https://doi.org/10.1029/2022JD037485

Khaykin, S., Podglajen, A., Ploeger, F., Grooß, J.-U., Tence, F., Bekki, S., et al. (2022). Global perturbation of stratospheric water and aerosol burden by Hunga eruption. *Commun. Earth Environ.*, *3*, 1–15. https://doi.org/10.1038/s43247-022-00652-x

Kloss, C., Sellitto, P., Renard, J.-B., Baron, A., Bègue, N., Legras, B., et al. (2022). Aerosol characterization of the stratospheric plume from the volcanic eruption at Hunga Tonga 15 January 2022. *Geophysical Research Letters*, *49*(16), e2022GL099394. https://doi.org/10.1029/2022GL099394

Lambert, A., Santee, M. L., & Livesey, N. J. (2016). Interannual variations of early winter Antarctic polar stratospheric cloud formation and nitric acid observed by CALIOP and MLS. *Atmospheric Chemistry and Physics*, *16*(23), 15219–15246. https://doi.org/10.5194/acp-16-15219-2016

Legras, B., Duchamp, C., Sellitto, P., Podglajen, A., Carboni, E., Siddans, R., et al. (2022). The evolution and dynamics of the Hunga Tonga–Hunga Ha'apai sulfate aerosol plume in the stratosphere. *Atmospheric Chemistry and Physics*, *22*, 14957–14970. https://doi.org/10.5194/acp-22-14957-2022

Li, C., Peng, Y., Asher, E., Baron, A. A., Todt, M., Thornberry, T. D., et al. (2024). Microphysical simulation of the 2022 Hunga volcano eruption using a sectional aerosol model. *Geophysical Research Letters*, *51*(11), e2024GL108522. https://doi.org/10.1029/2024GL108522

Luo, B., Krieger, U. K., & Peter, T. (1996). Densities and refractive indices of H2SO4/HNO3/H2O solutions to stratospheric temperatures. *Geophysical Research Letters*, *23*(25), 3707–3710. https://doi.org/10.1029/96GL03581

Manney, G. L., Santee, M. L., Lambert, A., Millán, L. F., Minschwaner, K., Werner, F., et al. (2023). Siege in the southern stratosphere: Hunga Tonga-Hunga Ha'apai water vapor excluded from the 2022 Antarctic polar vortex. *Geophysical Research Letters*, *50*(14), e2023GL103855. https://doi.org/10.1029/2023GL103855

Millán, L., Santee, M. L., Lambert, A., Livesey, N. J., Werner, F., Schwartz, M. J., et al. (2022). The Hunga Tonga-Hunga Ha'apai hydration of the stratosphere. *Geophysical Research Letters*, *49*(13), e2022GL099381. https://doi.org/10.1029/2022GL099381

19448007, 2024, 22, Downloaded from https://agupubs.onlinelibrary.wiley.com/doi/10.1029/2024GL111388 by Ripon College Lane Library, Wiley Online Library on [20/12/2024]. See the Terms and Conditions (https://onlinelibrary.wiley.com/terms-and-conditions) on Wiley Online Library for rules of use; OA articles are governed by the applicable Creative Commons License

Mills, M. J., Schmidt, A., Easter, R., Solomon, S., Kinnison, D. E., Ghan, S. J., et al. (2016). Global volcanic aerosol properties derived from emissions, 1990–2014, using CESM1(WACCM). *Journal of Geophysical Research: Atmospheres*, *121*(5), 2332–2348. https://doi.org/10.1002/2015JD024290

Norgren, M., Kalnajs, L. E., & Deshler, T. (2024). Measurements of total aerosol concentration in the stratosphere: A new balloon-borne instrument and a report on the existing measurement record. *Journal of Geophysical Research: Atmospheres*, *129*(14), e2024JD040992. https://doi.org/10.1029/2024JD040992

Proud, S. R., Prata, A. T., & Schmauß, S. (2022). The January 2022 eruption of Hunga Tonga-Hunga Ha'apai volcano reached the mesosphere. *Science*, *378*(6619), 554–557. https://doi.org/10.1126/science.abo4076

Sellitto, P., Podglajen, A., Belhadji, R., Boichu, M., Carboni, E., Cuesta, J., et al. (2022). The unexpected radiative impact of the Hunga Tonga eruption of 15th January 2022. *Commun. Earth Environ.*, *3*, 1–10. https://doi.org/10.1038/s43247-022-00618-z

Steele, H. M., & Hamill, P. (1981). Effects of temperature and humidity on the growth and optical properties of sulphuric acid—Water droplets in the stratosphere. *Journal of Aerosol Science*, *12*, 517–528. https://doi.org/10.1016/0021-8502(81)90054-9

Taha, G. (2022). OMPS-NPP L3 LP Aerosol Extinction Vertical Profile 5 x 15 deg lat-lon grid multi-wavelength monthly V1, Greenbelt, MD, USA, [Dataset]. *Goddard Earth Sciences Data and Information Services Center (GES DISC)*, https://doi.org/10.5067/BXR8K06YPR6U

Taha, G., Loughman, R., Colarco, P. R., Zhu, T., Thomason, L. W., & Jaross, G. (2022). Tracking the 2022 Hunga Tonga-Hunga Ha'apai aerosol cloud in the upper and middle stratosphere using space-based observations. *Geophysical Research Letters*, *49*(19), e2022GL100091. https://doi.org/10.1029/2022GL100091

Witze, A. (2022). Why the Tongan eruption will go down in the history of volcanology. *Nature*, *602*(7897), 376–378. https://doi.org/10.1038/d41586-022-00394-y

Wohltmann, I., Santee, M. L., Manney, G. L., & Millán, L. F. (2024). The chemical effect of increased water vapor from the Hunga Tonga-Hunga Ha'apai eruption on the Antarctic ozone hole. *Geophysical Research Letters*, *51*(4), e2023GL106980. https://doi.org/10.1029/2023GL106980

Zhang, J., Kinnison, D., Zhu, Y., Wang, X., Tilmes, S., Dube, K., & Randel, W. (2024). Chemistry contribution to stratospheric ozone depletion after the unprecedented water-rich Hunga Tonga eruption. *Geophysical Research Letters*, *51*(7), e2023GL105762. https://doi.org/10.1029/2023GL105762

Zhou, X., Dhomse, S. S., Feng, W., Mann, G., Heddell, S., Pumphrey, H., et al. (2024). Antarctic vortex dehydration in 2023 as a substantial removal pathway for Hunga Tonga-Hunga Ha'apai water vapor. *Geophysical Research Letters*, *51*(8), e2023GL107630. https://doi.org/10.1029/2023GL107630

Zhu, Y., Bardeen, C. G., Tilmes, S., Mills, M. J., Wang, X., Harvey, V. L., et al. (2022). Perturbations in stratospheric aerosol evolution due to the water-rich plume of the 2022 Hunga-Tonga eruption. *Commun. Earth Environ.*, *3*, 1–7. https://doi.org/10.1038/s43247-022-00580-w

19448007, 2024, 22, Downloaded from https://agupubs.onlinelibrary.wiley.com/doi/10.1029/2024GL111388 by Ripon College Lane Library, Wiley Online Library on [20/12/2024]. See the Terms and Conditions (https://onlinelibrary.wiley.com/terms-and-conditions) on Wiley Online Library for rules of use; OA articles are governed by the applicable Creative Commons License